

Strong-Coupling Features Due to Quasiparticle Interactions in Two Dimensional Superconductors

D. Coffey

Department of Physics, State University of New York, Buffalo, New York 14260

(February 1, 2008)

I calculate the effect of interactions among superconducting quasiparticles in two-dimensional(2D) a superconductor at $T=0$. The strength of the effective interaction among the quasiparticles is essentially given by the screened Coulomb interaction which has strength at low frequency because of the gapless nature of the plasmon. This is in contrast to three dimensions where the effective interaction has negligible weight at frequencies $\sim \Delta$, the superconducting gap. The quasiparticle interactions give rise to strong-coupling effects in experimental quantities which are beyond the conventional Eliashberg treatment of superconductivity. The present calculation offers an explanation of why these effects are much larger in 2D than in 3D superconductors and, in particular, why the analogous strong-coupling effects due to quasiparticle interactions are seen in data on the quasi-2D cuprate superconductors. the strong-coupling features seen in data on the cuprates are discussed in light of the present calculation.

I. INTRODUCTION

The BCS theory of superconductivity and its extension Eliashberg theory describe the electronic properties of the superconducting state in terms of self-energies which arise from the interaction of the superconducting quasiparticles with a boson which provides the mechanism for superconductivity [1,2]. It is assumed that the direct Coulomb interaction among the quasiparticles leads to renormalizations of the quasiparticle effective mass and lifetime in the normal state but that these renormalizations are unaffected by the superconducting transition. Within this approximation direct interactions among the superconducting quasiparticles are ignored and the only indication of interactions in the superconducting state are the $\alpha^2 F(\omega)$ strong-coupling features which appear in tunneling experiments and measurements of optical conductivity. The $\alpha^2 F(\omega)$ function then gives information on the density of the bosons and the strength of interaction with the quasiparticles. This has proved to be a very successful treatment of the properties of conventional superconductors where this mean field approximation for the direct long-range Coulomb interaction is justified by data. Models for the mechanism of high T_c superconductivity are based on the magnetic properties arising from strong short range Coulomb correlations as described in the Hubbard model. Treatments of these models also frequently assume that the normalizations determined in the normal state are unaffected by the transition to superconductivity.

However quasiparticle interactions in the ordered state have been shown to renormalize the superconducting gap, change the temperature dependence of the gap, and lead to finite quasiparticle lifetimes [3–7]. In the cuprate superconductors quasiparticle interactions lead to a feature in tunneling conductance across a superconductor-insulator-superconductor(g_{SIS}) junction at 3Δ in addition to the peak at 2Δ expected from the mean field approximation [8,9]. It is the scaling of the dip feature with Δ which distinguishes these corrections from the usual features in $\alpha^2 F(\omega)$ associated with the electron-phonon interaction. This scaling was originally demonstrated by comparing the tunneling conductance curves for a set of cuprate superconductors whose T_c 's varied from 5K to 100K [8]. More recently the intrinsic nature of this strong-coupling feature was demonstrated by comparing the tunneling conductance for $\text{Bi}_2\text{Sr}_2\text{CaCu}_2\text{O}_{8+\delta}$ as a function of doping and seeing the dip feature scale with the position of the 2Δ peak [9]. The size of the dip feature is much larger than the conventional electron-phonon corrections in the cuprates. This dip feature has been seen in the tunneling results of a number of groups [10–14] and the corresponding feature in the spectral density has also been identified in ARPES(Angle Resolved Photoemission Spectroscopy) data on $\text{Bi}_2\text{Sr}_2\text{CaCu}_2\text{O}_{8+\delta}$ [15–17] and has recently generated a renewed interest [18,19].

The magnitude of these corrections to the mean field treatment of superconductivity in the cuprates distinguishes the cuprates from conventional superconductors. Corrections to the mean field approximation, although present in conventional superconductors, do not in general lead to experimentally detected features. In this paper I argue that it is the low-dimensionality of the cuprate superconductors which is responsible for the comparatively large effects of quasiparticle interactions in the cuprates compared to conventional 3D superconductors. In low dimensional

systems fluctuations lead to the destruction of long-range order. In one dimension quantum fluctuations of the order parameter are sufficient to destroy long-range order [20] and in two-dimensions thermal fluctuations destroy the order [21,22]. Given this the effects of quantum fluctuations on superconducting properties would be expected to be more important in 2D than in 3D. This is investigated using a model Hamiltonian for 2D and 3D s-wave superconductors at zero temperature which includes the Coulomb interaction between electrons and the pairing interaction originally introduced by BCS which is characterized by a magnitude V_0 for electrons within an energy ω_D of the Fermi surface.

In this paper I show how the long-range nature of the Coulomb interaction leads to a qualitative difference in the quasiparticle properties of 2D and 3D s-wave superconductors. As Anderson [23] pointed out the long-range nature of the Coulomb interaction leads to the disappearance of the gapless mode associated with the phase of the superconductor order parameter in three dimensions and collective mode becomes the plasmon at energies much higher the energy scale of superconductivity. As a result the collective mode has no influence on superconducting properties [24–27]. This is not the case in two dimensions where the collective mode remains gapless just as the plasmon mode does for the 2D electron gas [28–33]. This leads to the possibility for the collective mode having a strong influence on quasiparticle properties unlike the case in three dimensions. Interactions among electrons are described by the Coulomb interaction and the pairing interaction responsible for the s-wave superconductivity in the generalized random phase approximation. I show that the quasiparticle interactions in the 2D superconductor are stronger than in the 3D case and that this difference can be traced to the low lying collective mode and the enhanced magnitude of the effective interaction at low frequencies compared to that in 3D.

Most models of the electronic properties of the cuprate superconductors have emphasized their layered nature and have employed 2D or quasi-2D Hamiltonians. These models have stressed short-range correlations either through an on-site Hubbard repulsion, in the weak or strong-coupling limits, or phenomenologically through residual short-range antiferromagnetic order which survives in the doped materials [35,36]. In these models a tight-binding bandstructure is used with either an on-site Hubbard repulsion coming from the weak-coupling side or the $t - J$ model coming from the strong-coupling side. Both approaches have been shown to be consistent with the $d_{x^2-y^2}$ symmetry of the order parameter. The importance of long-range correlations coming from the Coulomb interaction in quasi-2D systems, such as the layered cuprate superconductors, have not been considered in these treatments but potentially have a strong influence on the properties of quasi-2D superconductors.

The single-particle self-energies are calculated here for 2D and 3D s-wave superconductors and it is found that their magnitude in 2D is roughly ten times the value in 3D. The single-particle self-energies also have a stronger frequency dependence in 2D than in 3D which leads to stronger signatures of quasiparticle interactions in the spectral density and in the tunneling conductance of 2D superconductors compared to those in 3D superconductors. I calculate the strong-coupling corrections in model s-wave superconductor introduced and discuss how these results are related to experimental data on the cuprates. The paper is organized as follows. In section II the model is introduced. In section III the nature of the collective modes and their coupling to quasiparticle excitations are reviewed. The calculated single-particle self-energies are discussed in section IV and the influence of quasiparticle interactions on measured quantities is discussed in section V. The implications of the results presented here for work on the properties of the cuprates are discussed in section VI. A preliminary report of this work has appeared elsewhere [37].

II. MODEL

The starting point of the present analysis is a Hamiltonian, Eq.(1), describing a system of fermions interacting via a potential, $U(\vec{q})$.

$$H = \sum_{\vec{k}, \sigma} \xi_{\vec{k}} c_{\vec{k}\sigma}^\dagger c_{\vec{k}\sigma} + \frac{1}{2} \sum_{\vec{k}', \vec{k}, \vec{q}, \sigma} V(\vec{k}, \vec{q}) c_{\vec{k}-\vec{q}\sigma}^\dagger c_{-\vec{k}'+\vec{q}-\sigma}^\dagger c_{-\vec{k}'-\sigma} c_{\vec{k}\sigma} + \frac{1}{2} \sum_{\vec{k}', \vec{k}, \vec{q}, \alpha, \beta} U(\vec{q}) c_{\vec{k}-\vec{q}\alpha}^\dagger c_{-\vec{k}'+\vec{q}\beta}^\dagger c_{-\vec{k}'\beta} c_{\vec{k}\alpha} \quad (1)$$

where $\xi_{\vec{k}} = \frac{|\vec{k}|^2}{2m} - \frac{k_F^2}{2m}$, k_F is the Fermi momentum, $U(\vec{q}) = \frac{2\pi e^2}{\epsilon_s |\vec{q}|}$, ϵ_s is the static dielectric constant of the material and $V(\vec{k}, \vec{q})$ is the same pairing interaction as introduced by BCS, $V(\vec{k}, \vec{q}) = -V_0 \Theta(w_D - |\xi_{\vec{k}}|) \Theta(w_D - |\xi_{\vec{k}-\vec{q}}|)$, with $\Theta(x) = 0$ for $x < 0$ and $= 1$ for $x > 0$. w_D is a cutoff energy for the pairing interaction, which is a free parameter in the current calculation, was taken to be the Debye energy by BCS. Assuming that the ground state of the system at low temperatures is an s-wave superconductor, there is a transformation of the Hamiltonian to one written in terms of the quasiparticle operators, $\hat{\gamma}_{\vec{k}\sigma}$, which destroy this state. Transforming the Hamiltonian it is written in terms of these quasiparticle operators, $\hat{\gamma}_{\vec{k}\sigma}^\dagger$ and $\hat{\gamma}_{\vec{k}\sigma}$, the quasiparticle spectrum, $E_{\vec{p}} = \sqrt{\xi_{\vec{p}} + \Delta^2}$, and the coherence factors,

$u_p^2 = 1 - v_p^2 = \frac{1}{2}(1 + \frac{\xi_p}{E_p})$. Δ is determined by the weak coupling gap equation. The Hamiltonian becomes

$$H = \sum_{\vec{k}\sigma} E_{\vec{k}} \gamma_{\vec{k}\sigma}^\dagger \gamma_{\vec{k}\sigma} + H_C^{(R)} + H_C^{(L)} + H_C^{(3)} + H_C^{(4)} + H_P^{(phase)} + H_P^{(amp)} + H_P^{(3)}. \quad (2)$$

The terms in the Hamiltonian from the Coulomb interaction are,

$$H_C^{(R)} = \sum_{\vec{k}_1, \vec{k}_2, \vec{q}} U(\vec{q}) m(\vec{k}_1 + \vec{q}, \vec{k}_1) m(\vec{k}_2 + \vec{q}, \vec{k}_2) \gamma_{\vec{k}_1 + \vec{q}\uparrow}^\dagger \gamma_{-\vec{k}_1\downarrow}^\dagger \gamma_{-\vec{k}_2\downarrow} \gamma_{\vec{k}_2 + \vec{q}\uparrow}, \quad (3)$$

$$H_C^{(L)} = \frac{1}{2} \sum_{\vec{k}_1, \vec{k}_2, \vec{Q}, \sigma, \sigma'} U(\vec{k}_1 - \vec{k}_2) n(\vec{Q} - \vec{k}_1, \vec{Q} - \vec{k}_2) n(\vec{k}_1, \vec{k}_2) \gamma_{\vec{Q} - \vec{k}_1\sigma}^\dagger \gamma_{\vec{k}_1\sigma'}^\dagger \gamma_{\vec{k}_2\sigma'} \gamma_{\vec{Q} - \vec{k}_2\sigma}, \quad (4)$$

$$H_C^{(3)} = \sum_{\vec{k}_1, \vec{k}_2, \vec{q}, \sigma} U(\vec{q}) n(\vec{k}_1 + \vec{q}, \vec{k}_1) m(\vec{k}_2 - \vec{q}, \vec{k}_2) \gamma_{\vec{k}_1 - \vec{q}\sigma}^\dagger \gamma_{\vec{k}_2 + \vec{q}\uparrow}^\dagger \gamma_{-\vec{k}_2\downarrow}^\dagger \gamma_{\vec{k}_1\sigma} + h.c., \quad (5)$$

$$H_C^{(4)} = \frac{1}{2} \sum_{\vec{k}_1, \vec{k}_2, \vec{q}} U(\vec{q}) m(\vec{k}_1 + \vec{q}, \vec{k}_1) m(\vec{k}_2 - \vec{q}, \vec{k}_2) \gamma_{\vec{k}_1 + \vec{q}\uparrow}^\dagger \gamma_{-\vec{k}_1\downarrow}^\dagger \gamma_{\vec{k}_2 - \vec{q}\uparrow}^\dagger \gamma_{-\vec{k}_2\downarrow}^\dagger + h.c. \quad (6)$$

In the $H_C^{(R)}$ the net momentum of the two quasiparticles is the same as that in the Coulomb interaction. The $H_C^{(L)}$ term describes the scattering of pairs of quasiparticles whose net momentum \vec{Q} is different from that in the Coulomb interaction and appears in the calculation of ladder diagrams with the Coulomb interaction. The $H_C^{(4)}$ term describes the creation or destruction of two pairs of quasiparticles one with momentum \vec{q} and the other with momentum $-\vec{q}$ in which \vec{q} is also the momentum carried in the Coulomb interaction. The functions $l(\vec{k}_1, \vec{k}_2)$, $m(\vec{k}_1, \vec{k}_2)$, $n(\vec{k}_1, \vec{k}_2)$ and $p(\vec{k}_1, \vec{k}_2)$ are the usual combinations of coherence factors [38],

$$\begin{aligned} m(\vec{k} + \vec{q}, \vec{k}) &= u_{\vec{k} + \vec{q}} v_{-\vec{k}} + v_{\vec{k} + \vec{q}} u_{-\vec{k}}, \\ n(\vec{k} + \vec{q}, \vec{k}) &= u_{\vec{k} + \vec{q}} u_{\vec{k}} - v_{\vec{k} + \vec{q}} v_{\vec{k}}, \\ l(\vec{k} + \vec{q}, \vec{k}) &= u_{\vec{k} + \vec{q}} u_{-\vec{k}} + v_{\vec{k} + \vec{q}} v_{-\vec{k}}, \\ p(\vec{k} + \vec{q}, \vec{k}) &= u_{\vec{k} + \vec{q}} v_{-\vec{k}} - v_{\vec{k} + \vec{q}} u_{-\vec{k}}. \end{aligned} \quad (7)$$

The terms from the pairing interaction are,

$$H_P^{(phase)} = \frac{V_0}{2} \sum_{\vec{k}_1, \vec{k}_2, \vec{q}} l(\vec{q} + \vec{k}_1, \vec{k}_1) l(\vec{q} + \vec{k}_2, \vec{k}_2) \left[\gamma_{\vec{k}_1 + \vec{q}\uparrow}^\dagger \gamma_{-\vec{k}_1\downarrow}^\dagger - \gamma_{-\vec{k}_2\downarrow} \gamma_{\vec{k}_2 + \vec{q}\uparrow} \right] \left[\gamma_{\vec{k}_1 + \vec{q}\uparrow}^\dagger \gamma_{-\vec{k}_1\downarrow}^\dagger - \gamma_{-\vec{k}_2\downarrow} \gamma_{\vec{k}_2 + \vec{q}\uparrow} \right] \quad (8)$$

$$H_P^{(amp)} = \frac{V_0}{2} \sum_{\vec{k}_1, \vec{k}_2, \vec{q}} n(\vec{q} + \vec{k}_1, \vec{k}_1) n(\vec{q} + \vec{k}_2, \vec{k}_2) \left[\gamma_{\vec{k}_1 + \vec{q}\uparrow}^\dagger \gamma_{-\vec{k}_1\downarrow}^\dagger + \gamma_{-\vec{k}_2\downarrow} \gamma_{\vec{k}_2 + \vec{q}\uparrow} \right] \left[\gamma_{\vec{k}_1 + \vec{q}\uparrow}^\dagger \gamma_{-\vec{k}_1\downarrow}^\dagger + \gamma_{-\vec{k}_2\downarrow} \gamma_{\vec{k}_2 + \vec{q}\uparrow} \right] \quad (9)$$

$$H_P^{(2)} = \frac{V_0}{2} \sum_{\vec{k}_1, \vec{k}_2, \vec{Q}, \sigma, \sigma'} \left[u_{\vec{k}_1 + \vec{Q}} v_{-\vec{k}_1} v_{\vec{k}_2 + \vec{Q}} u_{-\vec{k}_2} + v_{\vec{k}_1 + \vec{Q}} u_{-\vec{k}_1} u_{\vec{k}_2 + \vec{Q}} v_{-\vec{k}_2} \right] \gamma_{\vec{Q} - \vec{k}_1\sigma}^\dagger \gamma_{\vec{k}_1\sigma'}^\dagger \gamma_{\vec{k}_2\sigma'} \gamma_{\vec{Q} - \vec{k}_2\sigma}, \quad (10)$$

$$H_P^{(3)} = V_0 \sum_{\vec{k}_1, \vec{k}_2, \vec{q}, \sigma} \left[u_{\vec{k} + \vec{q}} u_{\vec{k}} v_{\vec{k} + \vec{q}} u_{-\vec{k}} - v_{\vec{k} + \vec{q}} u_{-\vec{k}} u_{\vec{k} + \vec{q}} v_{-\vec{k}} \right] \gamma_{\vec{k}_1 - \vec{q}\sigma}^\dagger \gamma_{\vec{k}_2 + \vec{q}\uparrow}^\dagger \gamma_{-\vec{k}_2\downarrow}^\dagger \gamma_{\vec{k}_1\sigma} + h.c. \quad (11)$$

The $H_P^{(phase)}$ and $H_P^{(amp)}$ terms generate phase and amplitude fluctuations of the order parameter.

In normal ordering the $\gamma_{\vec{k}\sigma}^\dagger$ and $\gamma_{\vec{k}\sigma}$ operators terms quadratic in the new operators as well as terms without operators are generated from the kinetic energy and interaction terms. Considering first these terms from the kinetic energy and pairing interaction they include the effect of the pairing interaction calculated in the Hartree approximation. Ignoring the shift in the chemical potential due to the pairing interaction and using the weak-coupling gap equation these terms give the kinetic energy term, $\sum_{\vec{k}\sigma} E_{\vec{k}} \gamma_{\vec{k}\sigma}^\dagger \gamma_{\vec{k}\sigma}$, in the transformed Hamiltonian. Consequently in calculating the effect of the interactions in Equation(2) all contributions which include Hartree contributions to the quasiparticle lines from the pairing interaction should be dropped to avoid double-counting.

The quadratic terms arising in the normal ordering of the Coulomb parts of the Hamiltonian lead to the Hartree-Fock spectrum. In the normal state in 3D this leads to a large shift in the chemical potential, $\delta\mu = -\frac{e^2 k_F}{\pi}$, and a logarithmically diverging effective mass [39]. In 2D the self-energy leading to the Hartree-Fock spectrum is $\Sigma_{2D}^X(k) = \frac{-2e^2 k_F}{\pi} E(\frac{k}{k_F})$ for $k < k_F$ and $\Sigma_{2D}^X(k) = \frac{-2e^2 k_F}{\pi} [E(\frac{k_F}{k}) - (1 - (\frac{k_F}{k})^2) K(\frac{k_F}{k})]$ for $k > k_F$, where $K(x)$ and $E(x)$ are elliptic integrals of the first and second kind. As in 3D there is a large shift in the chemical potential, $\delta\mu = -\frac{2e^2 k_F}{\pi}$ and the effective mass diverges logarithmically. These results for the Coulomb interaction in the Hartree Fock approximation are strongly effected by higher order terms in the perturbation expansion and the long range interactions should be screened [40,41]. The statically screened Coulomb interaction leads to a smaller shift in the chemical potential and to a modest reduction in the effective mass. In the calculations discussed in the present paper the normal state quasiparticle spectrum is measured from the renormalized chemical potential and the reduction in the effective mass due to the statically screened Coulomb interaction is ignored. The single-particle self-energies for the $\gamma_{\vec{k}\sigma}^\dagger \gamma_{\vec{k}\sigma}$ and for the $\gamma_{\vec{k}\uparrow}^\dagger \gamma_{-\vec{k}\downarrow}^\dagger$ propagators are calculated at zero temperature using the generalized random phase approximation (GRPA). In this approximation the effective interaction is essentially the screened Coulomb interaction minus its static limit.

III. THE EFFECTIVE INTERACTION AND COLLECTIVE MODES

A. The Effective Interaction

The single-particle self-energies are calculated at zero temperature using the generalized random phase approximation (GRPA). In the GRPA ring diagrams, where each ring is the two quasiparticle propagator, are summed in which the vertices are dressed by the pairing interaction. In the absence of vertex corrections the two-quasiparticle propagator is

$$A_{00}(\vec{q}, \omega) = \sum_{\vec{k}} \frac{1}{2} \left(1 - \frac{\xi_{\vec{k}} \xi_{\vec{q}-\vec{k}}}{E_{\vec{q}-\vec{k}} E_{\vec{k}}} + \frac{\Delta^2}{E_{\vec{q}-\vec{k}} E_{\vec{k}}} \right) \frac{2(E_{\vec{q}-\vec{k}} + E_{\vec{k}})}{\omega^2 - (E_{\vec{q}-\vec{k}} + E_{\vec{k}})^2} \quad (12)$$

The interaction connecting the dressed two-quasiparticle propagators carries the net momentum and frequency of the two quasiparticles and is described by terms $H_C^{(R)}$ and $H_P^{(2)}$ in the Hamiltonian. However the magnitude of the pairing interaction is negligible compared to the Coulomb interaction and so $H_P^{(2)}$ can be ignored. Scaling energies with respect to Δ and momenta with respect to p_F , the strength of the interaction is given by a dimensionless parameter $\frac{2\pi e^2}{\epsilon_s p_F} N(0) = \frac{2}{\epsilon_s a_B p_F}$, where a_B is the Bohr radius. The strength of the effective interaction is determined by the product $\epsilon_s p_F$ which is a free parameter in the model.

At zero temperature the vertex corrections in the rings are given by the repeated scattering the two quasiparticles which is described by the $H_P^{(phase)}$ and the $H_P^{(amp)}$ terms in the Hamiltonian. Calculating a "rung" in this ladder sum by summing over the intermediate quasiparticle momenta, one finds

$$\left(B_{20}(\vec{q}, \omega) l(\vec{q} - \vec{k}_1, \vec{k}_1) l(\vec{q} - \vec{k}_2, \vec{k}_2) + C_{20}(\vec{q}, \omega) n(\vec{q} - \vec{k}_1, \vec{k}_1) n(\vec{q} - \vec{k}_2, \vec{k}_2) \right. \\ \left. + E_{20}(\vec{q}, \omega) \left[l(\vec{q} - \vec{k}_1, \vec{k}_2) n(\vec{q} - \vec{k}_2, \vec{k}_2) + l(\vec{q} - \vec{k}_1, \vec{k}_1) n(\vec{q} - \vec{k}_2, \vec{k}_2) \right] \right) \gamma_{\vec{q}+\vec{k}_1\uparrow}^\dagger \gamma_{\vec{k}_1\downarrow}^\dagger \gamma_{\vec{q}-\vec{k}_2\uparrow} \gamma_{\vec{k}_2\downarrow} \quad (13)$$

where

$$\begin{aligned}
B_{20}(\vec{q}, \omega) &= \sum_{\vec{k}} \frac{1}{2} \left(1 + \frac{\xi_{\vec{k}} \xi_{\vec{q}-\vec{k}}}{E_{\vec{q}-\vec{k}} E_{\vec{k}}} + \frac{\Delta^2}{E_{\vec{q}-\vec{k}} E_{\vec{k}}} \right) \frac{E_{\vec{q}-\vec{k}} + E_{\vec{k}}}{\omega^2 - (E_{\vec{q}-\vec{k}} + E_{\vec{k}})^2} \\
C_{20}(\vec{q}, \omega) &= \sum_{\vec{k}} \frac{1}{2} \left(1 + \frac{\xi_{\vec{k}} \xi_{\vec{q}-\vec{k}}}{E_{\vec{q}-\vec{k}} E_{\vec{k}}} - \frac{\Delta^2}{E_{\vec{q}-\vec{k}} E_{\vec{k}}} \right) \frac{E_{\vec{q}-\vec{k}} + E_{\vec{k}}}{\omega^2 - (E_{\vec{q}-\vec{k}} + E_{\vec{k}})^2} \\
E_{20}(\vec{q}, \omega) &= \sum_{\vec{k}} \frac{1}{2} \left(\frac{\xi_{\vec{k}}}{E_{\vec{k}}} + \frac{\xi_{\vec{q}-\vec{k}}}{E_{\vec{q}-\vec{k}}} \right) \frac{E_{\vec{q}-\vec{k}} + E_{\vec{k}}}{\omega^2 - (E_{\vec{q}-\vec{k}} + E_{\vec{k}})^2}
\end{aligned} \tag{14}$$

Summing over \vec{k} , $E_{20}(\vec{q}, \omega)$ vanishes with particle-hole symmetry. $B_{20}(\vec{q}, \omega)$ and $C_{20}(\vec{q}, \omega)$ are the phase and amplitude fluctuations of the order parameter, respectively. As a result of particle-hole symmetry these two channels are decoupled from one another and the ladder sum becomes

$$\left[\frac{V_0}{1 - V_0 B_{20}(\vec{q}, \omega)} l(\vec{q} - \vec{k}_1, \vec{k}_1) l(\vec{q} - \vec{k}_2, \vec{k}_2) + \frac{V_0}{1 - V_0 C_{20}(\vec{q}, \omega)} n(\vec{q} - \vec{k}_1, \vec{k}_1) n(\vec{q} - \vec{k}_2, \vec{k}_2) \right] \gamma_{\vec{q}+\vec{k}_1 \uparrow}^\dagger \gamma_{\vec{k}_1 \downarrow}^\dagger \gamma_{\vec{q}-\vec{k}_2 \uparrow} \gamma_{\vec{k}_2 \downarrow}. \tag{15}$$

This decoupling of amplitude fluctuations from charge fluctuations has been noted previously by Wu and Griffin [32].

The two different combinations of coherence factors in the phase and amplitude fluctuation channels, $l(\vec{q} - \vec{k}_1, \vec{k}_1)$ and $n(\vec{q} - \vec{k}_1, \vec{k}_1)$, lead to different couplings to the $H_C^{(R)}$ vertex which are given by a function $c_{20}(\vec{q}, \omega)$, for the phase fluctuations, and by $d_{20}(\vec{q}, \omega)$, for the amplitude fluctuations, where

$$\begin{aligned}
c_{20}(\vec{q}, \omega) &= \sum_{\vec{k}} \left(\frac{\Delta \omega}{E_{\vec{q}-\vec{k}} E_{\vec{k}}} \right) \frac{E_{\vec{q}-\vec{k}} + E_{\vec{k}}}{\omega^2 - (E_{\vec{q}-\vec{k}} + E_{\vec{k}})^2} \\
d_{20}(\vec{q}, \omega) &= \sum_{\vec{k}} \frac{(\xi_{\vec{k}} + \xi_{\vec{q}-\vec{k}}) \Delta}{E_{\vec{q}-\vec{k}} E_{\vec{k}}} \frac{E_{\vec{q}-\vec{k}} + E_{\vec{k}}}{\omega^2 - (E_{\vec{q}-\vec{k}} + E_{\vec{k}})^2}
\end{aligned} \tag{16}$$

The coupling of the $H_C^{(R)}$ to amplitude fluctuations of the order parameter is zero because of particle-hole symmetry. As discussed above the static part of the effective interaction leads to a renormalization of the chemical potential and the Hartree-Fock spectrum and is to be dropped assuming that energies are to be measured from the renormalized chemical potential. The effective interaction becomes

$$V_{eff}(\vec{q}, \omega) = \frac{U(\vec{q})}{1 - U(\vec{q})\Pi(\vec{q}, \omega)} - \frac{U(\vec{q})}{1 - U(\vec{q})P(\vec{q}, \omega = 0)} \tag{17}$$

where

$$\Pi(\vec{q}, \omega) = A_{00}(\vec{q}, \omega) - \frac{V_0 c_{20}^2(\vec{q}, \omega)}{1 - V_0 B_{20}(\vec{q}, \omega)} \tag{18}$$

Since the weak coupling gap equation, which determines the magnitude of Δ in the present calculation, is $1 = B_{20}(\vec{q} = 0, \omega = 0)$, $1 - V_0 B_{20}(\vec{q}, \omega)$ becomes $V_0 \delta B_{20}(\vec{q}, \omega)$, the V_0 factor cancels in Eq. (18), and there is no the explicit dependence of $\Pi(\vec{q}, \omega)$ on V_0 . Furthermore since the energies of interest here are $< 10\Delta$, $\epsilon_s p_F$ is the most important parameter and Δ sets the energy scale.

B. Collective Modes

Within this approximation, the imaginary part of the effective interaction is

$$V_{eff}''(\vec{q}, \omega) = U^2(q) \chi''(q, \omega) = \frac{U^2(\vec{q}) \Pi_A''(\vec{q}, \omega)}{[1 - U(\vec{q}) \Pi_A(\vec{q}, \omega)]^2} + U(\vec{q}) \delta[1 - U(\vec{q}) \Pi_A(\vec{q}, \omega)] \tag{19}$$

The second term gives the collective mode contribution. Collective modes have been investigated extensively for 3D superconductors [23–25] and more recently for 2D and quasi-2D superconductors [29–33]. As is well-known the energy of the collective mode in 3D superconductors is comparable to the plasma energy and the collective mode

has no influence on properties at energies $\sim \Delta$. On the other hand $\omega_{\vec{q}} = \sqrt{\frac{2\pi e^2 N(0)}{\Delta^2}} q$ at long wavelengths in 2D superconductors, where $N(0) = 4\pi m/h^2$. As a result $V_{eff}(\vec{q}, \omega)$ has an imaginary part given by $\pi Z_{\vec{q}} \delta(\omega - \omega_{\vec{q}})$ for values of $\omega \sim \Delta$, where $Z_{\vec{q}} = [U^2(\vec{q}) \frac{\partial \Pi_A(q, \omega)}{\partial \omega}]^{-1}|_{\omega=\omega_{\vec{q}}}$.

$V_{eff}''(\vec{q}, \omega)$ is $U^2(\vec{q})$ times the screened response function which is the dynamic structure factor, $S(q, \omega)$, calculated in the random phase approximation. Collective modes exhaust the f -sum rule, $\int d\omega \omega S(q, \omega) = \frac{Nq^2}{2m}$, at long wavelengths [34] so that

$$\int d\omega \omega S(q, \omega) \simeq Z_q \omega_q = \frac{Nq^2}{2m} \quad (20)$$

N is the number density of particles and the weight in the collective mode is $Z_q \simeq N \frac{q^2}{2m} \frac{1}{\omega_{\vec{q}}}$ in the long wavelength limit. As $\omega_{\vec{q}} \rightarrow 2\Delta$, $\omega_{\vec{q}}$ increases less rapidly than \sqrt{q} and is Landau damped in the two quasiparticle continuum. This is shown in figure 5 for $\epsilon_s p_F = 8\pi \text{\AA}^{-1}$. At the same time $Z_{\vec{q}}$ also starts to increase less rapidly than q^2 and eventually goes to zero as $\omega_{\vec{q}}$ reaches 2Δ .

In Figure 1 f_q is the fraction of the f -sum given by the collective, $f_q = Z_{\vec{q}} / \frac{Nq^2}{2m}$. When $\omega_{\vec{q}} \rightarrow 2\Delta$, $f_q \rightarrow 0$. At larger wavenumbers, the collective excitation reemerges as a resonance above the continuum. In the normal state when the collective mode, the plasmon, is calculated in the random phase approximation, the excitation is a pole of the response function at the same wavenumbers. However in the present calculation the imaginary part of $A_{00}(\vec{q}, \omega)$ behaves as $\sim N(0) \frac{\Delta^2}{\omega^2}$ at high frequencies. This is because the $\hat{\gamma}_{\vec{k}\sigma}$ operators are mixtures of $\hat{c}_{\vec{k}\sigma}$ and $\hat{c}_{\vec{k}-\sigma}^\dagger$ and so $A_{00}(\vec{q}, \omega)$ is a mixture of both normal state particle-hole and particle-particle propagators. Consequently there is a resonance at the plasmon energy rather than a pole.

In Figure 2 I show the plasmon resonance in $\chi''(\vec{q}, \omega)$ as a function of \vec{q} for $\epsilon_s p_F = 8\pi \text{\AA}^{-1}$. The important point about the effective interaction in two-dimensions is that there is weight at low frequencies comparable to Δ at long wavelengths. For example with $\epsilon_s p_F = 8\pi \text{\AA}^{-1}$, $\omega_{\vec{q}} < 10\Delta$ for $|\vec{q}| < 0.125 p_F$. As a result interactions between quasiparticles at low energies $\sim \Delta$ are much stronger than the interactions between the corresponding quasiparticles in 3D superconductors. As the value of $\epsilon_s p_F$ decreases the strength of the interaction increases and the resonance will emerge from the continuum at smaller q and ω . I will discuss the dependence of the results on $\epsilon_s p_F$ below.

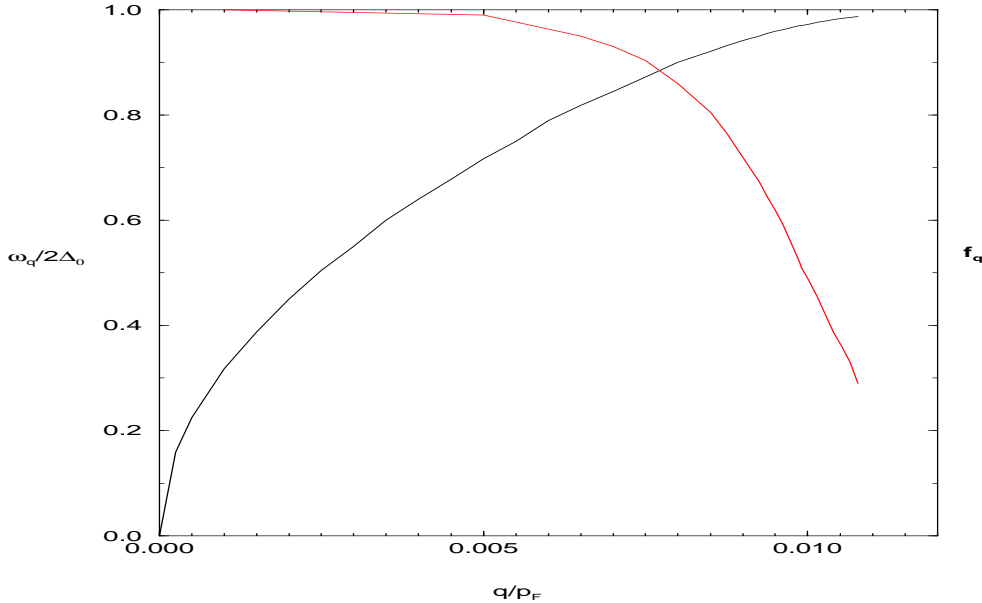


FIG. 1. Collective mode and weight in f -sum for $\Delta = 0.0273 e_F$. and $\epsilon_s p_F = 8\pi \text{\AA}^{-1}$.

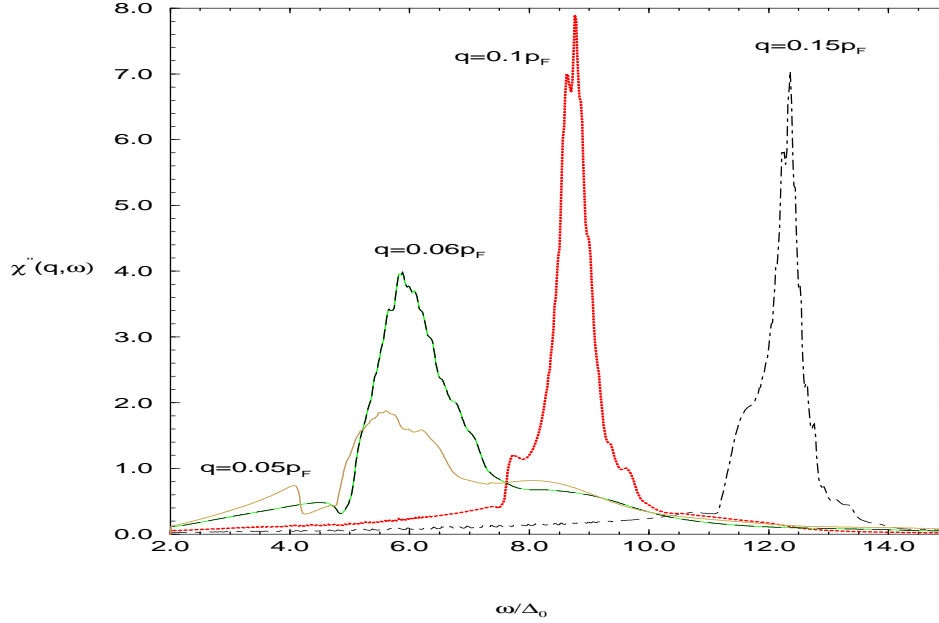


FIG. 2. Collective mode emerging from the continuum seen as a resonance in the imaginary part of the response function, $\chi''(q, \omega)$. As q increases the resonance appears at higher energies compared to Δ and becomes more like the normal state plasmon. Eventually it is Landau-damped in the quasiparticle continuum just the normal state plasmon.

Fertig and DasSarma [29] have calculated collective modes in layered superconductors allowing for hopping between planes. They found that collective modes exist in the gap for a limited range of momenta in the layers, $|\vec{q}|$, and transverse to the layers, q_z . This region of $|\vec{q}|$ and q_z values shrinks with increasing strength of the interlayer hopping, W . Interlayer hopping also leads to a gap in the collective mode dispersion at long wavelengths comparable in magnitude to W . The important feature of the collective mode spectrum from the point of view of the present work is that they are at energies of order Δ . As long as this is the case low energy quasiparticle interactions will be enhanced above those in 3D superconductors. Estimates given by Fertig and DasSarma suggest that this is the case in the cuprates. A detailed account of quasiparticle interactions in layered superconductors is in preparation [42].

IV. SINGLE-PARTICLE SELF-ENERGIES

The single-particle self-energy for the $\gamma_{\vec{k}_1\sigma}^\dagger \gamma_{\vec{k}_1\sigma}$ and $\gamma_{-\vec{k}_1\downarrow} \gamma_{\vec{k}_1\uparrow}$ propagators are calculated at zero temperature using the generalized random phase approximation (GRPA). The self-energies associated with the two single-particle propagators, $G_{\gamma^\dagger\gamma}(\vec{p}, iE_n)$ and $G_{\gamma\gamma}(\vec{p}, iE_n)$ are,

$$\begin{aligned} \Sigma_{\gamma^\dagger\gamma}(\vec{p}, iE_n) = & -\frac{1}{2} \sum_{\vec{q}} \left[\tanh\left(\frac{E_{\vec{p}-\vec{q}}}{2T}\right) [n^2(\vec{p}-\vec{q}, \vec{p}) V_e(\vec{q}, iE_n - E_{\vec{p}-\vec{q}}) - m^2(\vec{p}-\vec{q}, \vec{p}) V_e(\vec{q}, -iE_n - E_{\vec{p}-\vec{q}})] \right. \\ & \left. + \int_{-\infty}^{\infty} \frac{d\omega}{\pi} \coth\left(\frac{\omega}{2T}\right) V_e''(\vec{q}, \omega) \left[\frac{n^2(\vec{p}-\vec{q}, \vec{p})}{iE_n - \omega - E_{\vec{p}-\vec{q}}} + \frac{m^2(\vec{p}+\vec{q}, -\vec{p})}{iE_n + \omega + E_{\vec{p}-\vec{q}}} \right] \right] \end{aligned} \quad (21)$$

$$\begin{aligned} \Sigma_{\gamma\gamma}(\vec{p}, iE_n) = & -\frac{1}{2} \sum_{\vec{q}} \left[\tanh\left(\frac{E_{\vec{p}-\vec{q}}}{2T}\right) m(\vec{p}, \vec{p}-\vec{q}) n(\vec{p}, \vec{p}-\vec{q}) \times \left[V_e(\vec{q}, iE_n - E_{\vec{p}-\vec{q}}) - V_e(\vec{q}, -iE_n - E_{\vec{p}-\vec{q}}) \right] \right. \\ & \left. - \int_{-\infty}^{\infty} \frac{d\omega}{\pi} \coth\left(\frac{\omega}{2T}\right) V_e''(\vec{q}, \omega) \frac{\omega + E_{\vec{p}-\vec{q}}}{E_n^2 + (\omega + E_{\vec{p}-\vec{q}})^2} \right] \end{aligned} \quad (22)$$

Analytically continuing to the real axis and taking the zero temperature limit, the real part of the retarded self-energies are

$$\Sigma'_{\gamma^\dagger\gamma}(\vec{p}, E) = -\frac{1}{2} \sum_{\vec{q}} \left[n^2(\vec{p}-\vec{q}, \vec{p}) \left(V'_e(\vec{q}, -E - E_{\vec{p}-\vec{q}}) + \int_0^\infty \frac{d\omega}{\pi} \frac{2(E - E_{\vec{p}-\vec{q}}) V''_e(\vec{q}, \omega)}{(E - E_{\vec{p}-\vec{q}})^2 - \omega^2} \right) \right. \\ \left. - m^2(\vec{p}-\vec{q}, \vec{p}) \left(V'_e(\vec{q}, E + E_{\vec{p}-\vec{q}}) + \int_0^\infty \frac{d\omega}{\pi} \frac{2(E + E_{\vec{p}-\vec{q}}) V''_e(\vec{q}, \omega)}{(E + E_{\vec{p}-\vec{q}})^2 - \omega^2} \right) \right] \quad (23)$$

$$\Sigma'_{\gamma\gamma}(\vec{p}, E) = -\frac{1}{2} \sum_{\vec{q}} m(\vec{p}, \vec{p}-\vec{q}) n(\vec{p}, \vec{p}-\vec{q}) \\ \times \left(V'_e(\vec{q}, E - E_{\vec{p}-\vec{q}}) - V'_e(\vec{q}, -E - E_{\vec{p}-\vec{q}}) + \int_0^\infty \frac{d\omega}{\pi} \left[\frac{2(E - E_{\vec{p}-\vec{q}}) V''_e(\vec{q}, \omega)}{(E - E_{\vec{p}-\vec{q}})^2 - \omega^2} + \frac{2(E + E_{\vec{p}-\vec{q}}) V''_e(\vec{q}, \omega)}{(E + E_{\vec{p}-\vec{q}})^2 - \omega^2} \right] \right) \quad (24)$$

The imaginary parts of the self-energies are,

$$\Sigma''_{\gamma^\dagger\gamma}(\vec{p}, E) = \sum_{\vec{q}} \Theta(E - E_{\vec{p}-\vec{q}}) \frac{1}{2} \left(1 + \frac{\xi_{\vec{p}} \xi_{\vec{p}-\vec{q}} - \Delta^2}{E_{\vec{p}-\vec{q}} E_{\vec{p}}} \right) V''_{eff}(\vec{q}, E - E_{\vec{p}-\vec{q}}) \\ \Sigma''_{\gamma\gamma}(\vec{p}, E) = \sum_{\vec{q}} \Theta(E - E_{\vec{p}-\vec{q}}) \frac{(\xi_{\vec{p}} + \xi_{\vec{p}-\vec{q}}) \Delta}{E_{\vec{p}-\vec{q}} E_{\vec{p}}} V''_{eff}(\vec{q}, E - E_{\vec{p}-\vec{q}}), \quad (25)$$

where $V'_{eff}(\vec{q}, \omega)$ and $V''_{eff}(\vec{q}, \omega)$ are the real and imaginary parts of the effective interaction.

The calculated imaginary part of $\Sigma_{\gamma^\dagger\gamma}(\vec{p}, E)$ is shown for a two-dimensional s-wave superconductor in Figure 3 with $\epsilon_s p_F$ equal to $8\pi\text{\AA}^{-1}$,

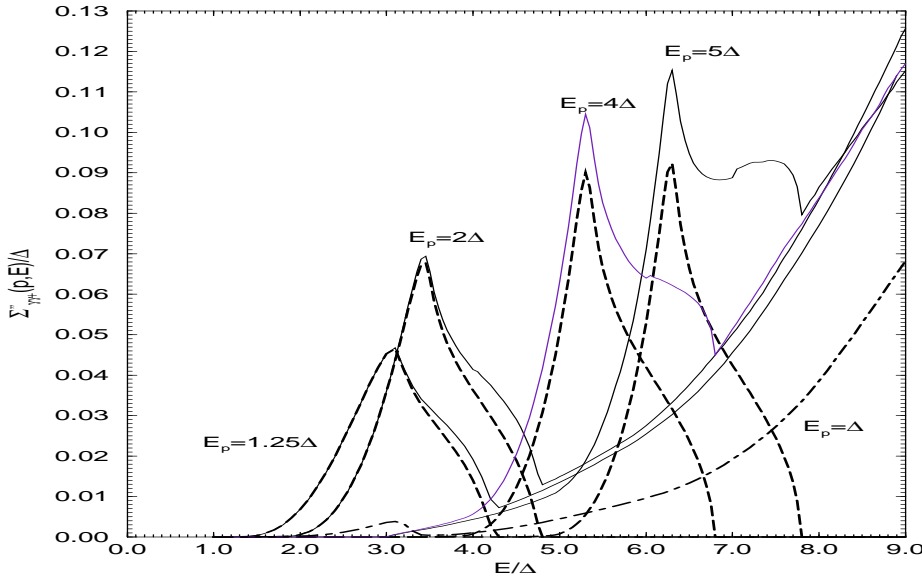


FIG. 3. Imaginary part of $\Sigma_{\gamma^\dagger\gamma}(\vec{p}, E)$ for a 2D s-wave superconductor for different values of E_p with $\epsilon_s p_F = 25.13\text{\AA}^{-1}$, $\omega_D = 0.1e_F$ and $\Delta = 0.0273e_F$. The dashed line is the contribution from the collective mode for each E_p . This is very small for $E_p = \Delta$ (dot-dash curve).

In Figure 3 the dashed curve is the contribution due to scattering off the collective mode and the solid line is the sum of the collective mode and continuum contributions. In 3D $\Sigma''_{\gamma\uparrow\gamma}(\vec{p}, E)$ increases monotonically with increasing $E > 3\Delta_0$ as the phase for decay into quasiparticle pairs increases. Comparing the 2D and 3D results one notes that the collective mode contribution is absent from the 3D case and that $\Sigma''_{\gamma\uparrow\gamma}(\vec{p}, E)$ is an order of magnitude larger in 2D. There is little dependence on $|\vec{p}|$ for $|\vec{p}| > 1.01p_F$ in the continuum contribution to $\Sigma''_{\gamma\uparrow\gamma}(\vec{p}, E)$. This contribution is a monotonically increasing function of energy at these low energies. The different coherence factors which appear in the expression for $\Sigma''_{\gamma\gamma}(\vec{p}, E)$ lead a smaller magnitude than for $\Sigma''_{\gamma\uparrow\gamma}(\vec{p}, E)$. However the energy dependence in the collective and continuum contributions are unchanged.

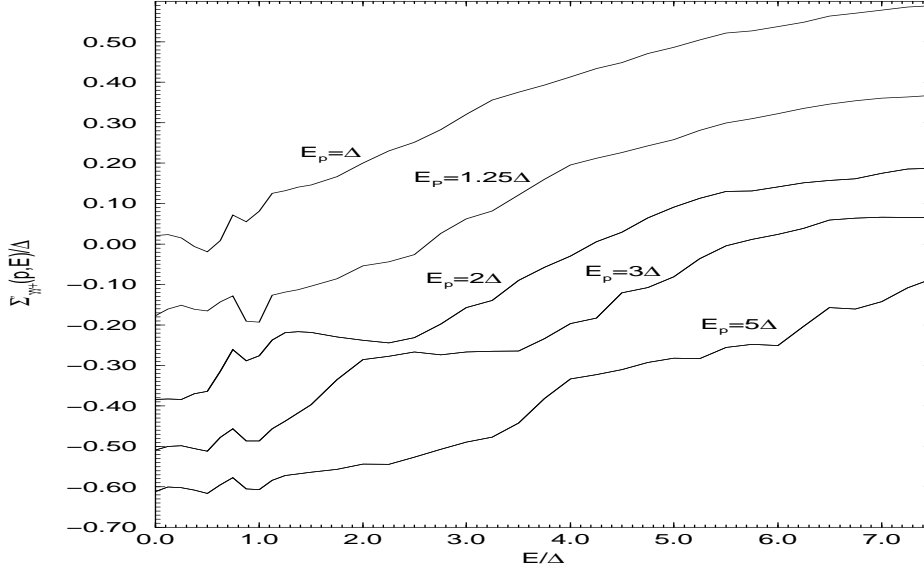


FIG. 4. Real part of the self-energy, $\Sigma_{\gamma\uparrow\gamma}(\vec{p}, E)$, for a 2D s-wave superconductor for different momenta with $\epsilon_s p_F = 25.13\text{\AA}^{-1}$, $\omega_D = 0.1e_F$ and $\Delta = 0.0273e_F$.

The real part of the $\Sigma_{\gamma\uparrow\gamma}(\vec{p}, E)$ self-energy is plotted for $\epsilon_s p_F = 8\pi\text{\AA}^{-1}$ in Figure 4 and for $\epsilon_s p_F = 4\pi\text{\AA}^{-1}$ in Figure 5. From Figure 4 one sees that the E dependence is different for $E < E_p$ where the dependence is non-monotonic, for $E \simeq E_p$ where there is very little dependence on E and for $E > E_p$, after a rapid increase, there is a monotonic almost linear increase with E . For $E \simeq 2\Delta$ this rapid increase has a step-like dependence.

In Figure 5 $\Sigma_{\gamma\uparrow\gamma}(\vec{p}, E)$ is seen to have the same form for different values of $\epsilon_s p_F$ but that the magnitude increases as $\epsilon_s p_F$ decreases, that is as the magnitude of the Coulomb interaction increases. For $E_p > 4\Delta$ the on-shell self-energy $\Sigma_{\gamma\uparrow\gamma}(\vec{p}, E = E_p)$ is only very weakly dependent on E and the magnitude is larger for smaller values of $\epsilon_s p_F$. For $\epsilon_s p_F = 8\pi\text{\AA}^{-1}$ $\Sigma'_{\gamma\uparrow\gamma}(\vec{p}, E_p) \rightarrow -0.3\Delta$, and for $\epsilon_s p_F = 4\pi\text{\AA}^{-1}$ $\Sigma'_{\gamma\uparrow\gamma}(\vec{p}, E_p) \rightarrow -0.78\Delta$, as $E \rightarrow 10\Delta$. For values of $\epsilon_s p_F$ such that $\Sigma'_{\gamma\uparrow\gamma}(\vec{p}, E_p) \simeq E_p$ for small E_p and corrections to GRPA should be calculated. A detailed discussion of the influence of the form of $\Sigma_{\gamma\uparrow\gamma}(\vec{p}, E)$ on the density of states and the tunneling conductance is given in the next section. The other self-energy, $\Sigma'_{\gamma\gamma}(\vec{p}, E)$, is shown for 2D in figures 6. The magnitude of this self-energy is smaller than the magnitude of $\Sigma'_{\gamma\uparrow\gamma}(\vec{p}, E_p) \simeq E_p$ and falls off monotonically for large E . Its magnitude also increases with decreasing $\epsilon_s p_F$ but its dependence on E remains unchanged.

Comparing the 2D and 3D cases again one finds that the magnitude of the real part of the self-energies is roughly an order of magnitude smaller in 3D than in 2D and for $E > \Delta_0$ the energy dependence is almost linear without the step feature of the 2D case. The same free parameter, $\epsilon_s p_F$, is present in the 3D calculations however because of the magnitude of the self-energies in 3D $\frac{\Sigma}{\Delta}$ remains small for much smaller values of $\epsilon_s p_F$.

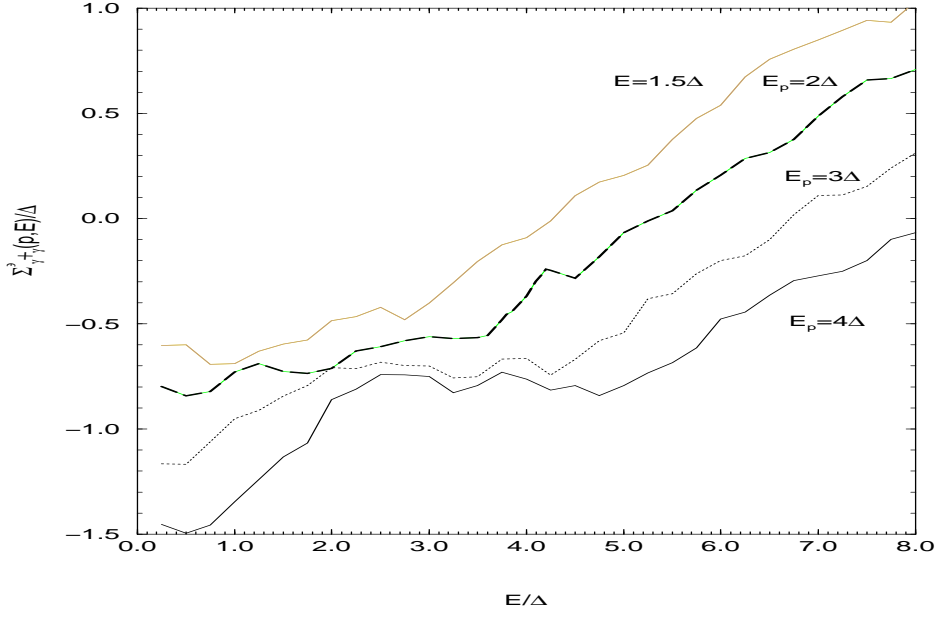


FIG. 5. Real part of the self-energy, $\Sigma_{\gamma\gamma}^r(\vec{p}, E)$, for a 2D s-wave superconductor for different momenta with $\omega_D = 0.1e_F$ and $\Delta = 0.0273e_F$. for $\epsilon_s p_F = 4\pi\text{\AA}^{-1}$. The dependence on E is the same as that for $\epsilon_s p_F = 8\pi\text{\AA}^{-1}$ but the magnitude is three times larger.

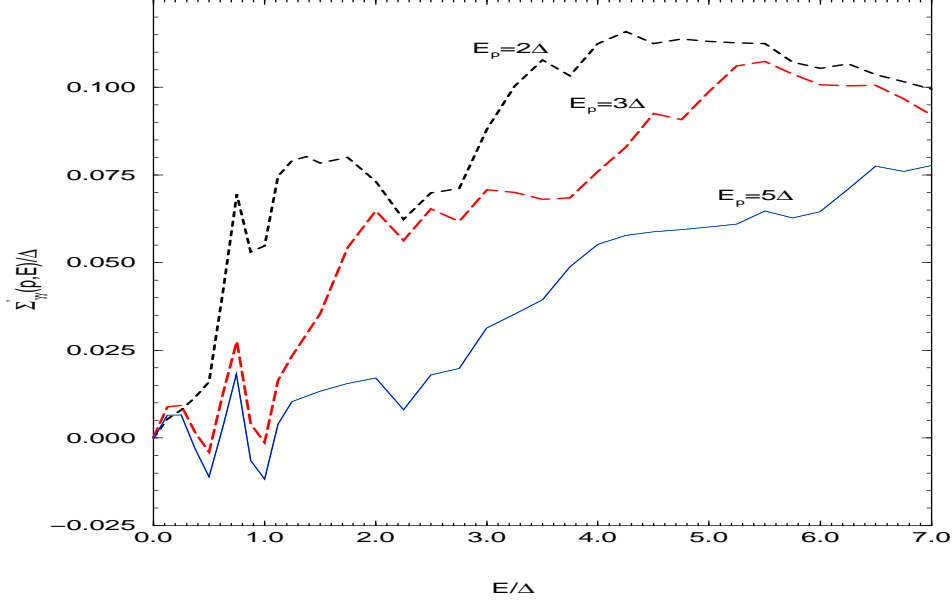


FIG. 6. Real part of the self-energy, $\Sigma_{\gamma\gamma}^r(\vec{p}, E)$, for a 2D s-wave superconductor for different momenta with $\epsilon_s p_F = 25.13\text{\AA}^{-1}$, $\omega_D = 0.1e_F$ and $\Delta = 0.0273e_F$.

The same calculation can be carried out for a 2D d-wave superconductor. In many models of superconductivity of the cuprates the d-wave symmetry arises from a pairing interaction with strong short-range correlations which are not present in this work. In a more complete treatment of the charge carriers in the cuprates both long range and short range parts of the Coulomb interaction would be included. As Hwang and Das Sarma [29] have pointed out the long range Coulomb interaction leads to quantitatively the same collective mode behavior in both s- and d- wave superconductors so that there is the same kind of enhancement of quasiparticle interactions in a 2D d-wave superconductor as appears in the 2D s-wave case. In calculations of superconducting properties for a d-wave superconductor with a tight-binding bandstructure bandstructure and gap anisotropy lead to anisotropy in the self-energy [6]. Nodes in the gap function also lead to damping of collective modes. These effects will not lead to a qualitatively different conclusion from the simple model discussed here but are clearly important for comparison with data on the cuprates.

V. STRONG COUPLING FEATURES IN TUNNELING CONDUCTANCES

Considering the expression for the the tunneling conductance across an superconductor-insulator-superconductor junction,

$$g = \frac{\partial I(V)}{\partial V} = \frac{\partial}{\partial V} \sum_{\vec{k}_1 \vec{k}_2} \int_0^{eV} d\omega A(\vec{k}_1, \omega) A(\vec{k}_2, eV - \omega) |T|^2 \quad (26)$$

where $I(V)$ is the current across an SIS junction and T is an unspecified matrix element between states on opposite sides of the junction which in principle depends on \vec{k}_1 and \vec{k}_2 . In this calculation the tunneling matrix elements are taken to be constants [43]. In describing tunneling in systems with strong bandstructure effects this approximation for the tunneling matrix element is not always justified [44]. Summing the carrier spins the spectral density $A(\vec{k}, \omega)$ is

$$A(\vec{k}, E) = \frac{2}{\pi} \left[\frac{u_{\vec{k}}^2 \Sigma''_{\gamma^\dagger \gamma}(\vec{k}, E)}{(E - E_{\vec{k}} - \Sigma'_{\gamma^\dagger \gamma}(\vec{k}, E))^2 + (\Sigma''_{\gamma^\dagger \gamma}(\vec{k}, E))^2} + \frac{v_{\vec{k}}^2 \Sigma''_{\gamma^\dagger \gamma}(-\vec{k}, -E)}{(E + E_{\vec{k}} + \Sigma'_{\gamma^\dagger \gamma}(-\vec{k}, -E))^2 + (\Sigma''_{\gamma^\dagger \gamma}(-\vec{k}, -E))^2} \right] \quad (27)$$

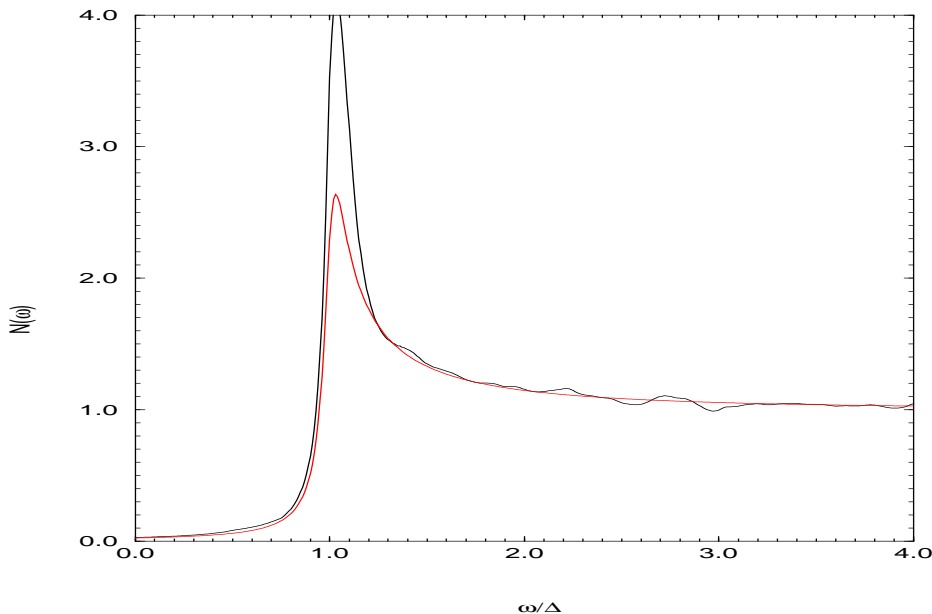


FIG. 7. Comparison between $N(\epsilon)$ with the mean field approximation, $N^{MF}(\epsilon)$ for 2D superconductors. $N^{MF}(\epsilon)$ was calculated using a Lorentzian with $\Gamma_0 = \Delta/20$.

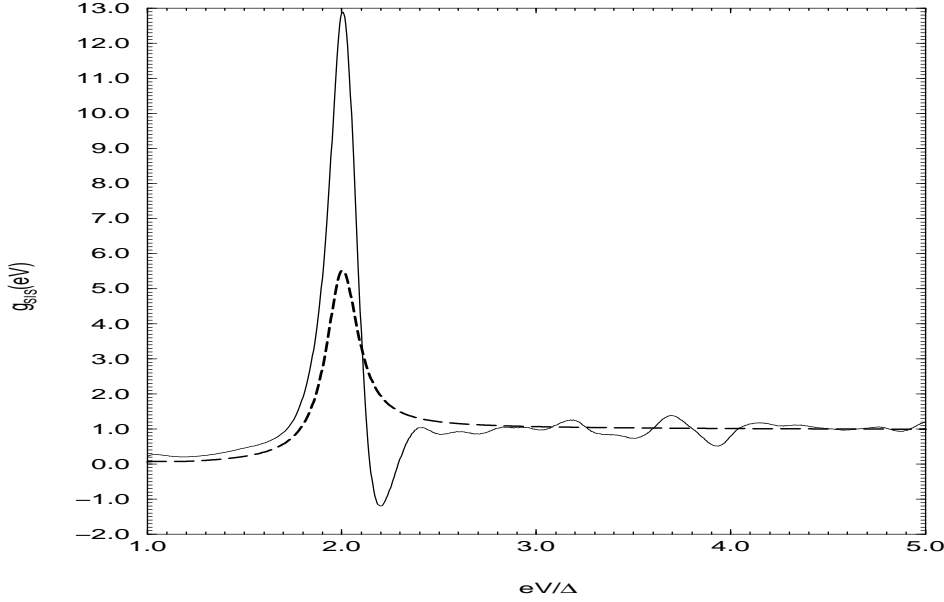


FIG. 8. Comparison between g_{SIS} corresponding to the $N(\omega)$ in Figure 7(a) with the mean field approximation g_{SIS}^{MF} (dashed curves), for 2D superconductors. $N^{MF}(\epsilon)$ was calculated using a Lorentzian with $\Gamma_0 = \Delta/20$.

The tunneling density of states, essentially the tunneling conductance across a superconductor-insulator-normal metal (SIN) junction, and the tunneling conductance are compared with the mean field approximation in Figure 7 and in Figure 8 for $\epsilon_s p_F = 8\pi\text{\AA}^{-1}$. There is a piling up of states at $E \sim \Delta$ due to $\Sigma'_{\gamma\dagger\gamma}(\vec{p}, E)$ compared to the density of states calculated in the mean field approximation, $N^{MF}(\omega) = \sum_{\vec{k}} \frac{\Gamma_0}{(\omega - E_{\vec{k}})^2 + \Gamma_0^2}$. In these calculations an extra damping term, $\Gamma_0 = \frac{\Delta_0}{20}$, is added to $\Sigma''_{\gamma\dagger\gamma}(\vec{p}, E)$ to mimic the effect of impurity scattering on these features. This piling up of states leads to a non-monotonic dependence of the current across an S-I-S junction as a function of applied voltage which in turn results the tunneling conductance shown in Figure 7. The large variation in $g_{SIS}(eV)$ at $eV \simeq 2\Delta$ comes from the magnitude of $\Sigma'_{\gamma\dagger\gamma}(\vec{p}, E)$.

The detailed E -dependence leads to strong-coupling effects which are seen at different frequencies in $N(\omega)$ and have corresponding features at frequencies shifted by Δ in $g_{SIS}(eV)$. These strong-coupling features are shown in the density of states and in the tunneling conductance in Figures 9 and 10 for different values of a phenomenological damping factor Γ_0 in the propagators. In this way some idea of the sensitivity of these features with damping can be seen. The magnitude of these features are at the 5% level in the density of states for $\Gamma_0 = \Delta/20$. The most prominent of these features are a bump feature between $\sim 2.6\Delta$ and 2.9Δ and the step feature at $\omega = 3\Delta$ in $N(\omega)$. These lead to more pronounced features at $eV = 4\Delta$ in $g_{SIS}(eV)$. This step feature is the analog of the dip feature seen in $g_{SIS}(eV)$ at $eV = 3\Delta$ in the d-wave cuprate superconductors whereas the bump feature comes from the collective mode contribution as will be discussed below. The origin of these features is the self-energy arising from quasiparticle interactions mediated by the screened Coulomb interaction and not from the pairing interaction.

The on-shell imaginary part of the self-energy, $\Sigma''_{\gamma\dagger\gamma}(\vec{p}, E_p)$, is given to a good approximation for $\epsilon_s p_F = 8\pi\text{\AA}^{-1}$ by

$$\Sigma''_{\gamma\dagger\gamma}(\vec{p}, E_p) = \Gamma_0 + 0.055\Theta(E_p - 3\Delta)[E_p - 3\Delta] \quad (28)$$

The small magnitude means that the spectral density at any momentum is to a very good approximation a Lorentzian and there is no structure from the energy dependence of $\Sigma_{\gamma\dagger\gamma}(\vec{p}, E)$ at values of E where the spectral density, $A(p, E)$, has any appreciable magnitude. If $\Sigma''_{\gamma\dagger\gamma}(\vec{p}, E)$ is set equal to $\Gamma_0 = \frac{\Delta}{20}$ and the conductance recalculated the same features appear in the tunneling conductance at the same energies. The only difference is that the new curve lies below the curve calculated with $\Sigma''_{\gamma\dagger\gamma}(\vec{p}, E)$. So the E dependence of $\Sigma''_{\gamma\dagger\gamma}(\vec{p}, E)$ is not responsible for the strong-coupling features in the density of states.

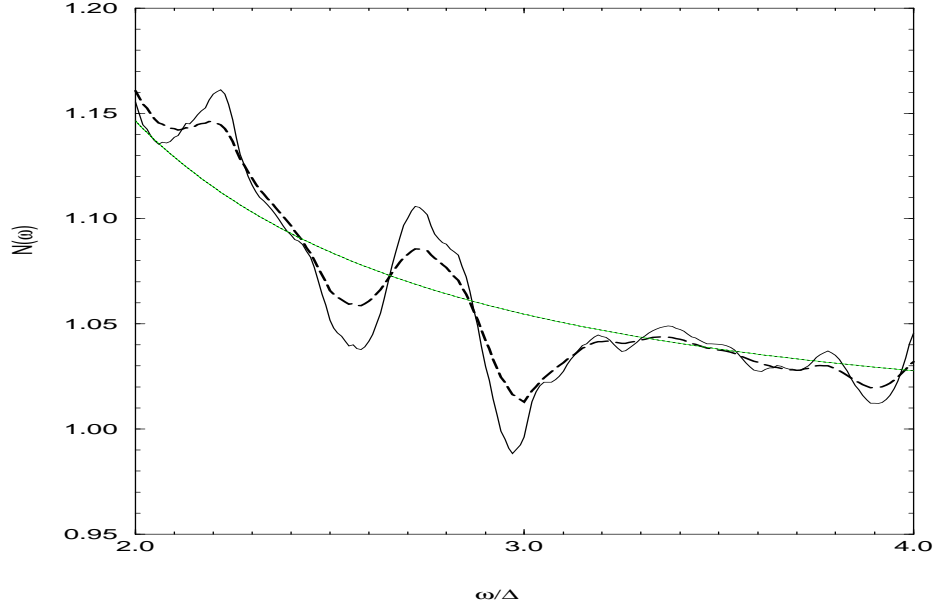


FIG. 9. Strong Coupling effects in the Density of States shown in Figure 7. The solid curve is the density of states calculated with $\Gamma_0 = \Delta/20$, the heavy dashed curve is calculated with $\Gamma_0 = \Delta/10$ and the dotted curve is the mean field density of states with $\Gamma_0 = \Delta/20$.

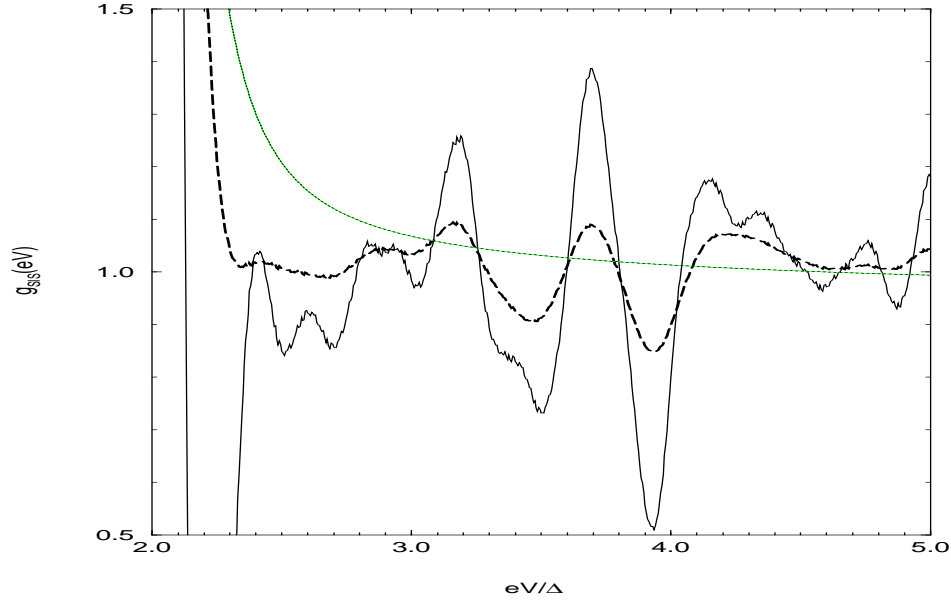


FIG. 10. Strong-coupling effects at $\omega = 4\Delta$ in g_{SIS} corresponding to that at $\omega = 3\Delta$ in the density of states shown in Figure 7. The solid curve is the case of $\Gamma_0 = \Delta/20$, the dashed curve is for $\Gamma_0 = \Delta/10$ and the dotted curve is the mean field curve with $\Gamma_0 = \Delta/20$.

The real part, $\Sigma'_{\gamma^\dagger\gamma}(\vec{p}, E)$, can be considered to the sum of two contributions, the on-shell piece, $\Sigma'_{\gamma^\dagger\gamma}(\vec{p}, E_p)$, and the energy dependent part, $\delta\Sigma'_{\gamma^\dagger\gamma}(\vec{p}, E)$. The position of the peak in the spectral density is given by

$$\omega_p = E_p + \Sigma'_{\gamma^\dagger\gamma}(\vec{p}, E_p) + \delta\Sigma'_{\gamma^\dagger\gamma}(\vec{p}, \omega_p) \quad (29)$$

ω_p is the renormalized quasiparticle spectrum. $\Sigma'_{\gamma^\dagger\gamma}(\vec{p}, E_p)/\Delta$ is plotted versus E_p/Δ in Figure 11(curve A). $\Sigma'_{\gamma^\dagger\gamma}(\vec{p}, E_p)$ has no strong dependence on E_p except in the region near $E_p = 3\Delta$ where the features are seen in the density of states. Beyond $E_p = 2\Delta$ it is a slowly increasing function of E_p except for these fluctuations. $\omega_p - E_p$ is plotted against ω_p in the same figure(curve B) and it is seen to have the same rapid variation near 3Δ . Comparing these curves with the density of states in Figure 9 the onset of the bump feature in the density of states at $\omega \simeq 2.6\Delta$ and the step feature at 3Δ can be seen to arise from structure of the quasiparticle spectrum. This structure in ω_p causes fluctuations in the density of states of the renormalized quasiparticle spectrum. Consequently the strong-coupling features in the density of states and the SIS tunneling arise from the momentum and energy dependence of $\Sigma'_{\gamma^\dagger\gamma}(\vec{p}, E)$ due to quasiparticle interactions.

The form of $\Sigma'_{\gamma^\dagger\gamma}(\vec{p}, \omega_p)$ comes from the continuum and collective contributions to the imaginary part of the self-energy, $\Sigma_{\gamma^\dagger\gamma}^{cont''}(\vec{p}, E)$ and $\Sigma_{\gamma^\dagger\gamma}^{coll''}(\vec{p}, E)$. From the Kramers-Kronig relation, the energy dependent real part of the self-energy is

$$\Sigma'_{\gamma^\dagger\gamma}(\vec{p}, \omega_p) = \frac{1}{\pi} \int_0^{\Omega_P} \frac{\Sigma_{\gamma^\dagger\gamma}^{cont''}(\vec{p}, E') dE'}{\omega_p - E'} + \frac{1}{\pi} \int_0^{\Omega_P} \frac{\Sigma_{\gamma^\dagger\gamma}^{coll''}(\vec{p}, E') dE'}{\omega_p - E'} + C_p \quad (30)$$

where C_p is the integral from the high energy cutoff, Ω_P , to infinity and over the negative energies which give only weak energy dependence.

In order to better understand the form of $\Sigma_{\gamma^\dagger\gamma}^{cont''}(\vec{p}, E)$ near $E = 3\Delta$, $\Sigma_{\gamma^\dagger\gamma}^{cont''}(\vec{p}, E)$ and $\Sigma_{\gamma^\dagger\gamma}^{coll''}(\vec{p}, E)$ can be approximated by simple analytic forms. From Figure 3 these can be approximate by $\Sigma_{\gamma^\dagger\gamma}^{cont''}(\vec{p}, E) = \alpha_p(E-3\Delta)\Theta(E-3\Delta)$ with $\alpha_p \simeq 0.055$. $\Sigma_{\gamma^\dagger\gamma}^{cont''}(\vec{p}, E)$ increases more rapidly than this linear function by $E \simeq 5\Delta$ but this approximation is sufficient to give a semi-quantitative account. I take $\Sigma_{\gamma^\dagger\gamma}^{coll''}(\vec{p}, E) = \beta_p\Theta(E_p+3\Delta-E)\Theta(E-E_p)f(E-E_p)$, where $f(E-E_p)$ is a function approximately the form of the energy dependence of the collective mode contribution. Looking at the form of the collective mode contribution in Figure 3 it can be approximated by $f(E-E_p) = (\frac{E-E_p}{\Delta})^2 \sqrt{\frac{E_p+3\Delta-E}{\Delta}}$. Taking this form and requiring that the maximum value of $\Sigma_{\gamma^\dagger\gamma}^{coll''}(\vec{p}, E)$ be 0.09Δ as in Figure 3 requires $\beta_p \simeq 0.02\Delta$ for $E_p > 3\Delta$. β_p grows from zero at $E_p = \Delta$ and is independent of E_p beyond $E_p = 3\Delta$.

Putting in the forms of the two contributions to the $\Sigma_{\gamma^\dagger\gamma}''(\vec{p}, E)$

$$\begin{aligned} \Sigma'_{\gamma^\dagger\gamma}(\vec{p}, E_p) &= \frac{\alpha_p}{\pi} \int_{3\Delta}^{\Omega_P} \frac{(E' - 3\Delta) dE'}{E_p - E'} + \frac{\beta_p}{\pi} \int_{E_p}^{E_p+3\Delta} \frac{f(E') dE'}{E_p - E'} + C_p \\ &= -\frac{\alpha_p}{\pi} (\Omega_P - 3\Delta) + \frac{\alpha_p}{\pi} (E_p - 3\Delta) \ln \frac{|E_p - 3\Delta|}{\Omega_P - 3\Delta} - \frac{\beta_p}{\pi} \frac{12\sqrt{3}}{5} + C_p \end{aligned} \quad (31)$$

and

$$\begin{aligned} \Sigma'_{\gamma^\dagger\gamma}(\vec{p}, \omega_p) &= \Sigma'_{\gamma^\dagger\gamma}(\vec{p}, E_p) + \frac{\beta_p}{\pi} \left[2(3)^{3/2} \frac{\omega_p - E_p}{\Delta} + \sqrt{3} \left(\frac{\omega_p - E_p}{\Delta} \right)^2 \ln \frac{|\omega_p - E_p|}{3\Delta} \right] \\ &\quad + \frac{\alpha_p}{\pi} \left[(\omega_p - 3\Delta) \ln \frac{|\omega_p - 3\Delta|}{\Omega_P - 3\Delta} - (E_p - 3\Delta) \ln \frac{|E_p - 3\Delta|}{\Omega_P - 3\Delta} \right] \end{aligned} \quad (32)$$

From Figure 11 it can be seen that $\delta\Sigma'_{\gamma^\dagger\gamma}(\vec{p}, \omega_p) \simeq 0.01\Delta$ so that $\omega_p - E_p \simeq \Sigma'_{\gamma^\dagger\gamma}(\vec{p}, E)$ giving

$$\begin{aligned} \Sigma'_{\gamma^\dagger\gamma}(\vec{p}, \omega_p) &\simeq \Sigma'_{\gamma^\dagger\gamma}(\vec{p}, E_p) \left(1 + 2(3)^{3/2} \frac{\beta_p}{\pi\Delta} \right) + \sqrt{3} \frac{\beta_p}{\pi} \left(\frac{\Sigma'_{\gamma^\dagger\gamma}(\vec{p}, E_p)}{\Delta} \right)^2 \ln \frac{|\Sigma'_{\gamma^\dagger\gamma}(\vec{p}, E_p)|}{3\Delta} \\ &\quad + \frac{\alpha_p}{\pi} \left[(\omega_p - 3\Delta) \ln \frac{|\omega_p - 3\Delta|}{\Omega_P} - (E_p - 3\Delta) \ln \frac{|E_p - 3\Delta|}{\Omega_P} \right] \end{aligned} \quad (33)$$

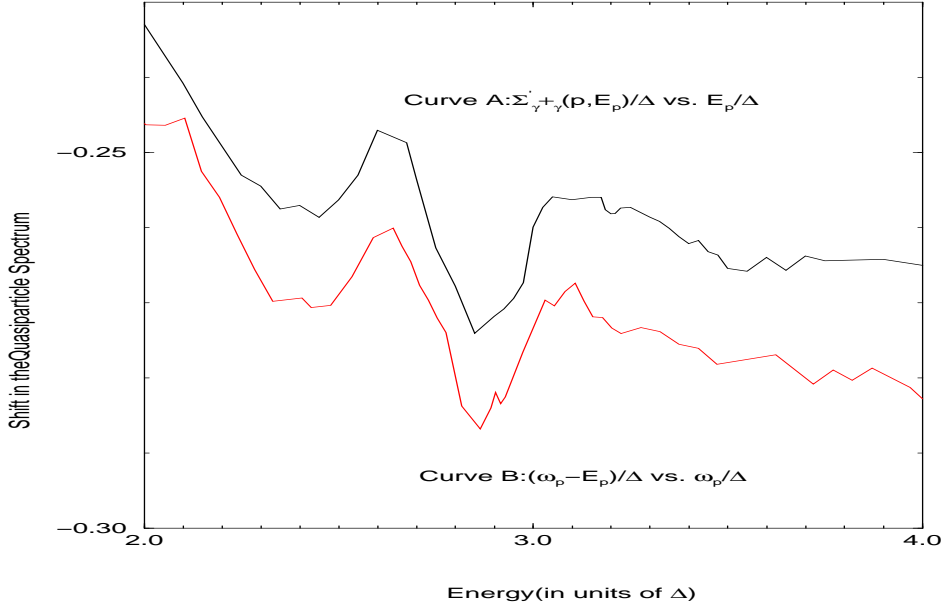


FIG. 11. The on-shell self-energy, Σ , as a function of E_p and the shift in the quasiparticle spectrum, ω_p^* from E_p as a function of ω_p^* for $\epsilon_s p_F = 25.13 \text{ \AA}^{-1}$, $\omega_D = 0.1 e_F$ and $\Delta = 0.0273 e_F$. The position of the features in the quasiparticle spectrum are seen to coincide with the frequencies at which the strong-coupling features are seen in the density of states.

Using β_p discussed above one finds from Equation (33) that the magnitude of $\Sigma'_{\gamma^\dagger\gamma}(\vec{p}, \omega_p)$ is enhanced over that of $\Sigma'_{\gamma^\dagger\gamma}(\vec{p}, E_p)$ by about 5%. Considering the simple form of the functions used this is consistent with the results shown in Figure 11. Taking Ω_p and α_p to be constants and allowing β_p to increase by about $\frac{1}{3}$ between $E_p = 2\Delta$ and for $E_p = 3\Delta$, consistent the calculation of $\Sigma''_{\gamma^\dagger\gamma}(\vec{p}, E)$, the form of $\Sigma'_{\gamma^\dagger\gamma}(\vec{p}, E_p)$ for $E_p \geq 2.5\Delta$ is seen to come from the combination of the $\frac{\alpha_p}{\pi}(E_p - 3\Delta)\ln\frac{|E_p - 3\Delta|}{\Omega_p}$ and the $\frac{\beta_p}{\pi}\frac{12\sqrt{3}}{5}$ terms. The weak features in curve B, $(\omega_p - E_p)/\Delta$ vs. ω_p/Δ , at $\omega_p = 3\Delta \pm \frac{1}{2}\Sigma'_{\gamma^\dagger\gamma}(\vec{p}, E_p)$ come from the term proportional to α_p in Equation (34) where the term in the brackets goes through maxima in magnitude. However a better approximation for the momentum and energy dependence of $\Sigma''_{\gamma^\dagger\gamma}(\vec{p}, E)$ is required beyond the form used here in order to recover the E_p dependence of $\Sigma'_{\gamma^\dagger\gamma}(\vec{p}, E_p)$ between $E_p = 2\Delta$ and $E_p = 2.5\Delta$ without a detailed fitting of the C_p and Ω_p functions. The β_p term coming from the collective contribution to $\Sigma''_{\gamma^\dagger\gamma}(\vec{p}, E)$ is responsible for the bump feature in $\Sigma'_{\gamma^\dagger\gamma}(\vec{p}, E_p)$ between $2.6\Delta < E < 3\Delta$. It is clear that without the collective mode contribution the bump in the density of states below $\omega = 3\Delta$ would be absent and the step at $\omega = 3\Delta$ would be more pronounced.

VI. DISCUSSION

As well as tunneling conductance and the density of states discussed here ARPES experiments can provide information on the single-quasiparticle spectral density once background has been taken into account. In the calculation discussed above the spectral density is a Lorentzian with no experimentally detectable non monotonic energy dependence away from the peak. Many-body effects give a non-trivial quasiparticle spectrum, ω_p , leading to the strong-coupling effects discussed above but do not lead to any signatures in ARPES measurement such as the dip feature at $\omega = 2\Delta$ in the cuprate superconductors. A necessary condition that features away from the quasiparticle peak in the spectral density lead to observable features in ARPES is that the imaginary part of the self-energy should have both a strong energy dependence and be sufficiently large that there is weight away the peak. In the present case the linear dependence of $\Sigma'_{\gamma^\dagger\gamma}(\vec{p}, E_p)$ on E_p and the small magnitude combine to ensure that the energy dependence of $\Sigma''_{\gamma^\dagger\gamma}(\vec{p}, E)$ leads to no features in ARPES or tunneling conductance.

This is in contrast to models used to describe ARPES and tunneling data in the cuprates [5,6,19] where the strong-coupling feature is at 2Δ in the density of states and the spectral density, as measured in ARPES, [17] and at 3Δ in the SIS tunneling conductance. In these models a phenomenological form for $\Sigma_{\gamma\uparrow\gamma}''(\vec{p}, E)$ is used in which there is a rapid increase in the magnitude of $\Sigma_{\gamma\uparrow\gamma}''(\vec{p}, E)$ to a value $\sim \Delta$ in some momentum directions at $E \simeq 2\Delta$ after which any dependence of $\Sigma_{\gamma\uparrow\gamma}''(\vec{p}, E)$ on E is weak. In these models $\Sigma_{\gamma\uparrow\gamma}'(\vec{p}, E)$ is assumed to lead only to a renormalization of the gap. This model for $\Sigma_{\gamma\uparrow\gamma}''(\vec{p}, E)$ in the case of a d-wave superconductor is suggested by Golden-rule calculation of the decay of mean field quasiparticles in a tight-binding bandstructure [5,6]. The results of the tight-binding calculations depend on both the chemical potential and the presence of next-nearest neighbor terms in the bandstructure. The form of $\Sigma_{\gamma\uparrow\gamma}''(\vec{p}, E)$ is consistent with that arising from low energy antiferromagnetic spin fluctuations [45]. The bandstructure and short-range correlations leading to low energy magnetic excitations which are responsible for the strong-coupling effects in the models of the cuprates are absent in the calculation reported here. However the present calculation points to the necessity of including long range Coulomb interaction in order to distinguish low dimensional from conventional superconductors and suggests that any model which is to quantitatively account for these features in the cuprates should incorporate the effects of long-range correlations as well as the short-range correlation associated with the magnetic properties of the cuprates. The extent to which a superconductor is low dimensional, where the effects discussed would be important, is determined in the model described here by the weight in the effective quasiparticle interaction due to the Coulomb interaction at low frequencies. In layered superconductors Das Sarma et al. [29,30] have shown that depending on interplanar coupling and on the direction of the wavevector the collective mode spectrum, $\omega_{\vec{q}}$, is at energies $\sim \Delta$ as $|\vec{q}| \rightarrow 0$. There should still be substantial weight in the collective mode at frequencies $< 10\Delta$ in order for quasiparticle interactions to be enhanced above the 3D case. This issue is presently being investigated [42].

Since the original identification of the dip feature in ARPES there have been suggestions that it is strongly associated with the mechanism for superconductivity in the cuprates. Arnold et al. [46] identified the strong-coupling features seen in the data of Dessau et al. [16]. with a “bosonic peak” which they proceeded to analyze in terms of the $\alpha^2 F(\omega)$ function of Eliashberg theory. Analysis of more recent data have lead Shen and Schrieffer [18] to a model where the quasiparticles are strongly coupled to a collective mode. This collective mode contributes to the line shape in ARPES in the normal state and is strongly influenced by the superconducting transition. In their picture the dip feature in the line shape is the consequence of the strong quasiparticle coupling to the collective mode which provides the pairing mechanism for hiT_c superconductivity. In the present case also the collective mode is strongly effected by the transition to superconducting ground state although it is not associated with the mechanism for superconductivity. It decays into pairs of superconducting quasiparticles once its energy reaches 2Δ , reemerges at higher energies and essentially follows the dispersion of the normal state plasmon. The contribution to off-shell self-energy, $\Sigma''(p, E)$, from scattering from the plasmon is very weak at the low energies, $\sim \Delta$, for the 2D electron gas. It leads to a weak feature in the spectral density even at $p = 1.1p_F$ which corresponds to $E_p \simeq 8\Delta$ for $\Delta = 0.0273e_F$ and would not be detected easily in experiment [47].

VII. CONCLUSIONS

In this paper I have shown how quantum fluctuations in 2D charged Fermi systems are enhanced over those in 3D. This result holds for both the normal and superconducting states. However in the superconducting state they clearly lead to strong-coupling features in experimental quantities which are a probe of the superconducting state.

In the model discussed in this paper the quasiparticle interaction responsible for the feature at $\omega = 3\Delta$ in SIN for s-wave superconductor and the corresponding feature at $\omega = 4\Delta$ in SIS is the Coulomb interaction and not the pairing interaction giving the s-wave superconducting ground state. In the absence of the Coulomb interaction the pairing interaction would produce the same feature but would not account for the difference in magnitude of these effects in conventional 3D superconductors and the quasi-2D cuprate superconductors. The anomalously large magnitude of the strong coupling features seen in the cuprates suggest that the electronic properties of these materials are quasi-2D. This is a basic assumption which most workers in the area have employed for a long time. However the long range part of the Coulomb interaction has been ignored. The present calculation suggests that, although the interactions which provide the mechanism for superconductivity in the cuprates may be short correlations, long range Coulomb correlations should also be included. In particular the pairing mechanism undoubtedly contributes to the magnitude of the feature at $\omega = 2\Delta$ in ARPES data and to the strong-coupling features seen in tunneling experiments at $eV = 3\Delta$ but they are unlikely to solely account for its magnitude.

-
- [1] P.B. Allen and B. Mitrović, “Theory of Superconducting T_c ” in *Solid State Physics -Advances in Research and Applications*, Vol. 37(Eds. H. Ehrenreich, F. Seitz and D. Turnbull), Academic Press, New York (1982), pg.2-92.
 - [2] J.P. Carbotte, “Properties of Boson-Exchange Superconductors”, *Rev. Mod. Phys.* **62**, 1027 (1990).
 - [3] A.R. Bishop, P.S. Lomdahl, J.R. Schrieffer and S.A. Trugman, *Phys. Rev. Lett.* **61**, 2709 (1988).
 - [4] D. Coffey, *Phys. Rev. B* **42**, 6040 (1990); **47**, 593 (1993).
 - [5] D. Coffey and L. Coffey, *Phys. Rev. Lett.* **70**, 1529 (1993).
 - [6] D. Coffey, *J. Phys. Chem. Sol.*, **54**, 1181 (1993).
 - [7] P. Monthoux and D.J. Scalapino, *Phys. Rev. Lett.* **72**, 1874 (1994).
 - [8] J.F. Zasadzinski, N. Tralshawla, P. Romano, Q. Huang, J. Chen and K.E. Gray, *J. Phys. Chem. Solids* **53**, 1635 (1992); J.F. Zasadzinski, Q. Huang, P. Romano and K.E. Gray, *Bull. Am. Phys. Soc.* **38**, 583 (1993).
 - [9] Y. De Wilde, N. Miyakawa, P. Guptasarma, M. Iavarone, L. Ozyuzer, J. F. Zasadzinski, P. Romano, D.G. Hinks, C. Kendziora, G. W. Crabtree and K. E. Gray, Preprint 1997.
 - [10] J.J. Wnuk, R.T.M. Smokers, F.W. Nolden, L.W. Streurs, Y.S. Wang, and H. van Kempen, *Supercond. Sci. Technol.* **4**, 412 (1991).
 - [11] D. Mandrus, L. Forro, D. Koeller and L. Mihaly, *Nature* **351**, 460 (1991); D. Mandrus, J. Hartge, L. Forro, C. Kendziora and L. Mihaly, *Europhysics Lett.* **22**, 199 (1993).
 - [12] Q. Chen and K.W. Ng, *Phys. Rev. B* **45**, 2569 (1992).
 - [13] J. Hartge, L.Forro, M.C. Martin, C. Kendziora and L. Mihaly, *J. Phys. Chem. Sol.* **54**, 1359 (1993).
 - [14] S.I. Vedeneev, A.G.M. Jansen, P. Samuely, V.A. Stepanov, A.A. Tsvetkov and P. Wyder, *Phys. Rev. B* **49**, 9823 (1994).
 - [15] Y. Hwu, L. Lozzi, M. Marsi, S. La Rosa, M. Winokur, P. Davis, M. Onellion, H. Berger, F. Gozzo, F. Levy and G. Margaritondo, *Phys. Rev. Lett.* **67**, 2573 (1991).
 - [16] D.S. Dessau, B.O. Wells, Z. X. Shen, W.E. Spicer, A.J. Arko, R.S. List, D.B. Mitzi and A. Kapitulnik, *Phys. Rev. Lett.* **66**, 2160 (1991).
 - [17] Z.-X. Shen D. S. Dessau, B. O. Wells, D. M. King, W. E. Spicer, A. J. Arko, D. Marshall, L. W. Lombardo, A. Kapitulnik, P. Dickinson, S. Doniach, J. DiCarlo, A. G. Loeser and C. H. Park, *Phys. Rev. Lett.* **70**, 1553 (1993).
 - [18] Z.-X. Shen and J.R. Schrieffer, *Phys. Rev. Lett.* **78**, 1771 (1997).
 - [19] M.R. Norman, H. Ding, J.C. Campuzano, T. Takeuchi, M. Randeria, T. Yokoya, T. Takehashi, T. Mochiku and K. Kadowaki, preprint, cond-mat/9702144.
 - [20] K.V. Efetov and A.I. Larkin, *Soviet Phys. JETP* **39**, 1129 (1974).
 - [21] T.M. Rice, *Phys. Rev.* **140**, A1889 (1965).
 - [22] P.C. Hohenberg, *Phys. Rev.* **158**, 383 (1967).
 - [23] P.W. Anderson, *Phys. Rev.* **112**, 1900 (1958).
 - [24] G. Rickayzen, *Phys. Rev.* **115**, 795 (1959).
 - [25] A. Bardasis and J.R. Schrieffer, *Phys. Rev.* **121**, 1050 (1961).
 - [26] R. E. Prange, *Phys. Rev.* **129**, 2495 (1963).
 - [27] P.C. Martin in *Superconductivity*, edited by R.D. Parks (Dekker, New York 1969).
 - [28] F.J. Dunmore, D.Z. Liu, H.D. Drew, Das Sarma, Q. Li and D.B. Fenner, *Phys. Rev. B* **52**, R731 (1995).
 - [29] H.A. Fertig and S. Das Sarma, *Phys. Rev. Lett.* **65**, 1482 (1990); H.A. Fertig and S. Das Sarma, *Phys. Rev. B* **51**, 15317 (1995).
 - [30] E.H. Hwang and S. Das Sarma, *Phys. Rev. B* **52**, 7010 (1995).
 - [31] R. Côte and A. Griffin, *Phys. Rev. B* **48**, 10404 (1993).
 - [32] W.-C. Wu and A. Griffin, *Phys. Rev. Lett.* **74**, 158 (1995); *Phys. Rev. B* **51**, 15317 (1995); and *Phys. Rev. B* **51**, 1190 (1995).
 - [33] D. van der Marel, *Phys. Rev. B* **51**, 1147 (1995).
 - [34] D. Pines and P. Nozières, “The Theory of Quantum Liquids”, (W.A. Benjamin, New York, 1966).
 - [35] D.J. Scalapino, *Phys. Rep.* **250**, 329 (1995).
 - [36] D. Pines, *Physica C* **235 - 240**, 113 (1994).
 - [37] D. Coffey, *Europhysics Lett.* preprint (cond-mat/9704133).
 - [38] J. R. Schrieffer, “Theory of Superconductivity”, (Addison-Wesley, Redwood City, California 1964), Chapter 3.
 - [39] G.D. Mahan, “Many-Particle Physics”, (Plenum Press, New York 1990), second edition, chapter 5.
 - [40] V. Khodel and V. R. Shaginyan, *JETP Lett.* **51**, 553 (1990).
 - [41] P. Nozières, *J. Phys. I* **2**, 443 (1992).
 - [42] D. Coffey, unpublished.
 - [43] M.H. Cohen, L.M. Falicov and J.E. Phillips, *Phys. Rev. Lett.* **8**, 316 (1962).
 - [44] L. Coffey, D. Lacy, K. Kouznetsov and A. Erner, *Phys. Rev. B* **52**, R731 (1995).
 - [45] P. Monthoux and D. Pines, *Phys. Rev. B* **47**, 6069 (1993).

- [46] G. B. Arnold, F. M. Mueller, and J. C. Swihart, Phys. Rev. Lett. **67**, 2569 (1991).
- [47] J.S. Kim and D. Coffey, Phys. Rev. B, in press, (cond-mat/9705065).